PASJ: Publ. Astron. Soc. Japan **44**, L135–L140 (1992)

High-Temperature Plasmas in Active Regions Observed with the Soft X-Ray Telescope aboard Yohkoh

Hirohisa HARA and Saku TSUNETA
Institute of Astronomy, The University of Tokyo, Mitaka, Tokyo 181
James R. LEMEN and Loren W. ACTON
Lockheed Palo Alto Research Laboratory, Palo Alto, CA 94304, U.S.A.
and
James M. MCTIERNAN
Space Sciences Laboratory, University of California, Berkeley, CA 94720, U.S.A.

(Received 1992 June 1; accepted 1992 July 27)

Abstract

High-temperature plasmas reaching 5–6 $\times$ 10^6 K in solar active regions have been found with the soft X-ray telescope aboard Yohkoh. NOAA region 6919 was investigated in detail using five different X-ray filters: The temperature of a bright loop in the active region is 5.7 $\times$ 10^6 K, with an emission measure of 5.0 $\times$ 10^{28} cm^{-5}; in a fainter part of the region plasma, we find 5.0 $\times$ 10^6 K and 4.0 $\times$ 10^{27} cm^{-5}. This indicates that such high-temperature plasmas exist in the active region, irrespective of the brightness. Another observation of the quiet corona was conducted in order to investigate the reliability of a temperature analysis with the same filter pairs which show such high temperatures in active regions: The inferred temperature was 2.7 $\times$ 10^6 K, and the emission measure 1.3 $\times$ 10^{26} cm^{-5}, which is consistent with the typical results of Skylab. Therefore, the high-temperature plasmas in solar active regions are considered to be real.

Key words: Plasmas — Sun: active regions — Sun: corona — Sun: X-rays

1. Introduction

The Soft X-ray Telescope (SXT) aboard Yohkoh (Tsuneta et al. 1991) is equipped with five X-ray analysis filters [Al 0.1 μm (hereafter thin Al or Al 0.1), AlMgMn-sandwich, Be 119 μm, Al 12 μm (thick Al or Al12), Mg 3 μm] on two rotatable filter wheels located in front of the CCD detector, providing a pixel-by-pixel temperature diagnostic capability. The filter wheel is controlled by a microprocessor, thus providing very versatile observing sequences. The normal filter sequence is optimized so that it provides the best temperature diagnostic capability. The temperatures and emission measures are obtained from images taken with two different broad-band X-ray filters, (*filter ratio method*, Vaiana et al. 1973; Gerassimenko and Nolte 1978). The excellent scattering performance of the SXT mirror provides high-resolution temperature and emission measure images. These images give crucial information concerning the energetics of the plasmas in the solar corona. In this paper we report the initial results of a temperature analysis of an active region with this instrument.

2. Filter Ratio Method

In this section we briefly summarize the *filter ratio method* (Hara 1992). The energy of photons (E_i) transformed into pairs of electrons and holes in a CCD pixel per unit time is described as

$$E_i = \frac{1}{4\pi D^2} \int_0^\infty \int_\lambda N_e^2(l) P[\lambda, T(l)] \eta_i(\lambda) d\lambda dl \cdot d\sigma, \quad (1)$$

where D is the distance between the Earth and the Sun; N_e is the electron density; $P(\lambda, T)$ is the emissivity (including both emission lines and continuum) as a function of the wavelength (λ) and the plasma temperature (T); $\eta(\lambda)$ is the telescope effective area, which is the product of the telescope aperture, the mirror reflectivity, the filter transmission, and the CCD quantum efficiency at wavelength (λ); l is the path length along the line of sight; $d\sigma$ is the area on the Sun corresponding to one image pixel; and i denotes the filter number. We used Mewe's spectral data (Mewe et al. 1985, 1986) for the emissivity $[P(\lambda, T)]$.

In the case of isothermal plasma, the above equation can be written as

$$E_i = \frac{1}{4\pi D^2} F_i(T) \varepsilon, \quad (2)$$

where

$$F_i = \int_\lambda P(\lambda, T)\eta_i(\lambda)d\lambda \quad (3)$$

and

$$\varepsilon = \int_0^\infty N_e^2(l)dl \cdot d\sigma. \quad (4)$$

Here, ε is the volume emission measure, while $\varepsilon/d\sigma$ is simply called the emission measure in this paper.

Since a photon energy of 3.65 eV is necessary for the creation of an electron-hole pair in the CCD, the number of the electrons (N_i) created per unit time is $N_i = E_i/3.65k_e$, where k_e is the conversion factor (1.6×10^{-12} erg eV^{-1}). We define DN (Data Number) as being a unit used to measure the number of electrons: since $1DN \equiv 100$ electrons, $DN_i = N_i\delta t_i/100$, where δt_i is the exposure duration. From the above equations DN_i can be expressed in terms of the plasma temperature (T) and the emission measure (ε) as

$$DN_i = f_i(T)\,\varepsilon\delta t_i. \quad (5)$$

The ratio (R_{ij}) of the images taken with two different filters (i and j) is written as

$$R_{ij} \equiv \frac{DN_i/\delta t_i}{DN_j/\delta t_j} = \frac{F_i(T)}{F_j(T)}. \quad (6)$$

Since equation (6) indicates that the ratio is only a function of the temperature, a plasma temperature can be derived by taking the filter ratio. Figure 1 shows the temperature dependence of the filter ratio for various filter pairs. The volume emission measure is derived from equation (5) using the temperature deduced from the filter ratio.

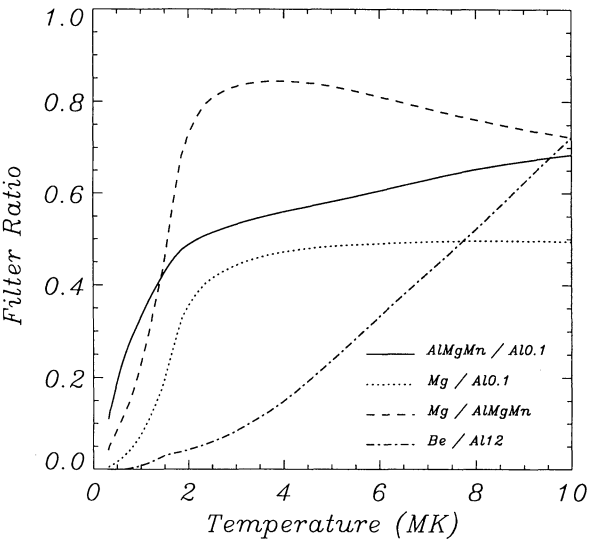

Fig. 1. SXT signal ratios for the representative filter pairs.

3. Temperature Analysis of an Active Region

NOAA region 6919, the brightest solar active region in X-rays on 1991 November 18 was observed with five X-ray filters for 30 min in the 5″ (3.6×10^3 km) resolution mode (figure 2). We derived the temperature of the central part of the bright loop (region A) as well as the faint part of the active region (region B) enclosed by the squares in figure 2. A C1 class flare had occurred in the brightest loop, including region A, about 20 min before the observation. It lasted for about 10 min, while region B did not change in intensity for at least 30 min.

Figures 3a and 3b show the temperatures derived from all possible filter pairs. The error bars correspond to a conservative 10% peak-to-peak systematic error assumed for the telescope sensitivity calibration. The photon statistical error is a factor of three less than the systematic error in this observation. The temperatures of regions A and B are concentrated around 6×10^6 K and 5×10^6 K, respectively. For instance, the temperature and emission measure from pairs of thick Al and Be filters are 5.7×10^6 K and 5.0×10^{28} cm^{-5} for region A, and 5.0×10^6 K and 4.0×10^{27} cm^{-5} for region B. Other pairs of 5–6 $\times 10^6$ K give almost identical emission measures in each region. Such high-temperature plasmas were found also in most of about 20 other bright active regions which we investigated. Although some of the filter pairs are not very sensitive at higher temperatures, the ratio of Be/Al12, for instance, shows a rather higher sensitivity at these temperature, as shown in figure 1, so that we can be confident concerning the existence of 5–6 $\times 10^6$ K plasmas.

On the other hand, the Mg/Al0.1, Mg/AlMgMn ratio shows T = 2–3 $\times 10^6$ K, which is systematically lower than those derived from above. The Mg/AlMgMn ratio shows two solutions, as given in figure 3 (cf. figure 1); the temperature at 6–8 $\times 10^6$ K was not found from pairs, including the thick Al and Be filters which have higher sensitivity at higher temperatures. It may therefore be reasonable to adopt the lower temperature solution at 2–3 $\times 10^6$ K. The emission measure at 2–3 $\times 10^6$ K is found to be 2.8×10^{29} cm^{-5} (region A) and 1.9×10^{28} cm^{-5} (region B), which is about 5-times larger than those at $T = 5$–6×10^6 K in both regions. Finally, the AlMgMn-sandwich/Al0.1 ratio shows an intermediate temperature, which may be a combined result of the two temperatures; it may also result from such an intermediate-temperature plasma.

Even if active region plasmas have multi-thermal components along the line of sight, each filter pair gives a single temperature which is the weighted mean of the

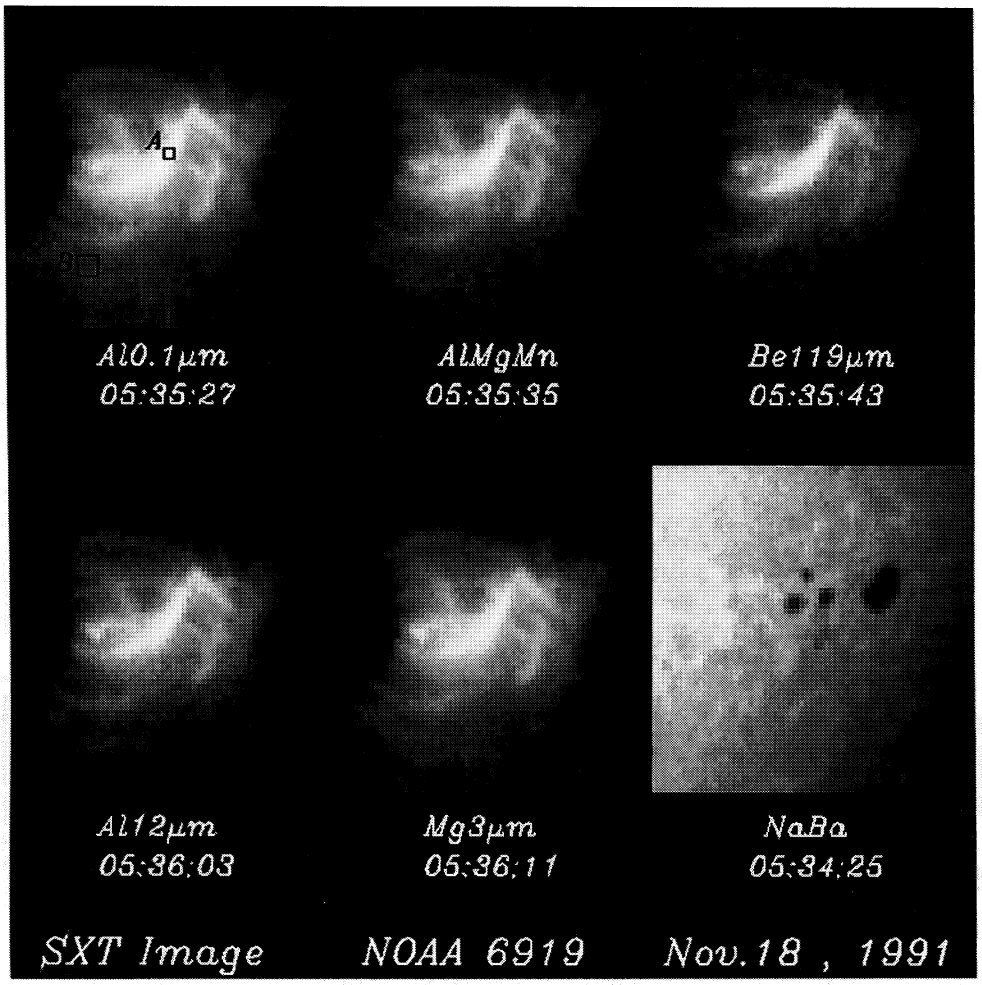

Fig. 2. Images of the NOAA 6919 region taken with five X-ray filters and the narrowband optical filter at each exposure time(UT). The spatial resolution is $5'' \times 5''$ (3.6×10^3 km square), and the field of view is $5'.4 \times 5'.4$ (2.3×10^5 km square).

differential distribution of the plasma temperatures with the filter response functions. Since the filters of thin Al, AlMgMn-sandwich and Mg are more sensitive to the plasma below 2×10^6 K, compared with thicker filters, such as thick Al and Be, the filter ratios from these filters give a larger weight to the cooler plasma, while the ratios from the other filter pairs are more sensitive to higher temperatures. Thus, the component obtained from the pair of thin Al and Mg is not artificial, but may indicate a distributed differential emission measure (DEM) in the active-region plasma.

Figure 4 shows the temperature and emission measure contour maps of the active region derived by the pair of thick Al and Be filters. (The analysis does not include faint regions, such as region B, because of poor photon statistics.) The distinct loop located at the center of the region has a higher emission measure compared with the surroundings, and the emission measure around the loop top is higher than at the footpoints. The temperatures of the coronal loops are higher than the surrounding region, and a variation of temperature along the coronal loop exists with a temperature difference of $\Delta T \sim 1 \times 10^6$ K. From this temperature gradient we estimate the conductive energy loss of region A to be 1.6×10^7 erg cm^{-2} s^{-1}. To estimate the radiative loss of region A, we assume that the path length along the line of sight is the same as half of the distance between the footpoints of the brightest loop including region A. The average density of region A is 3.3×10^9 cm^{-3} for a path length $l = 5.0 \times 10^9$ cm; and the radiative loss is thus 4.5×10^5 erg cm^{-2} s^{-1}. The cooling time scale of region A is therefore determined by conduction rather than radiation.

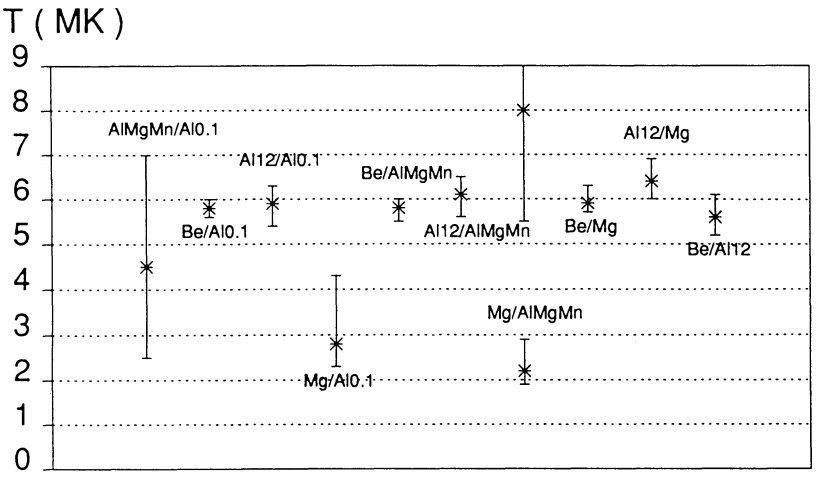

(a)

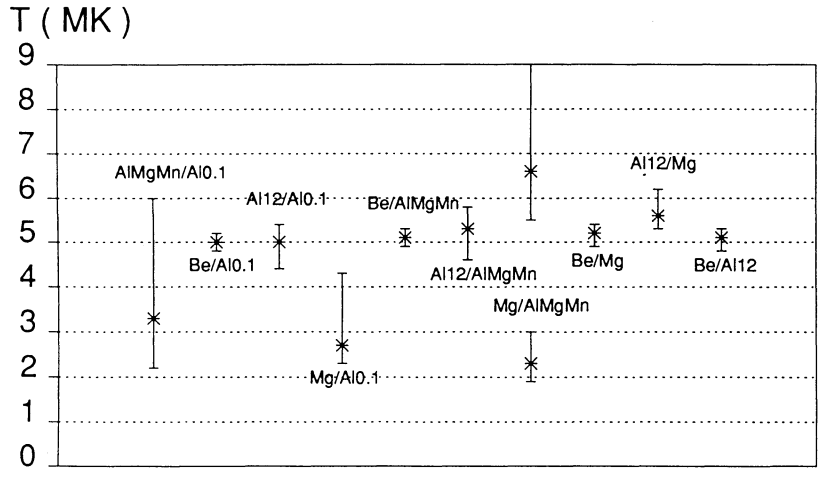

(b)

Fig. 3. Temperature of regions A (a) and region B (b) derived by using various filter pairs. AlMgMn/Al refers to the temperatures derived from a pair of the AlMgMn-sandwich filter and the thin Al filter. The vertical bars correspond to the 10% peak-to-peak systematic error in the telescope sensitivity calibration. There is no special meaning in the horizontal direction.

4. Discussion

Another observation of the quiet corona was specifically performed on 1992 January 21, in order to investigate the capability of temperature analysis with SXT. The temperature and emission measure of the quiet corona deduced from thin Al and thick Al filters were 2.7×10^6 K and 1.3×10^{26} cm^{-5}, respectively. These are consistent with the results of Raymond and Doyle (1981). We can thus say that the hot components in the active region are due to the real temperature structure of the active region. Another check regarding the temperature analysis capability was performed by using the GOES data collected on the same day. The temperature and volume emission measure from the GOES data (Thomas et al. 1985) were 4.0×10^6 K and 1.4×10^{49} cm^{-3}, while those by the integrated SXT whole Sun images taken with thin Al and Be filters were 4.5×10^6 K and 1.3×10^{49} cm^{-3}, respectively. Although the GOES data are more reliable regarding higher temperatures, this agreement is rather satisfactory.

As discussed above, high temperature plasmas of $5\text{–}6 \times 10^6$ K were found in the active region, NOAA 6919. The hot material is distributed even in faint parts of the active region, such as region B, which had not participated in the C1 flare. This suggests that the hot material exists

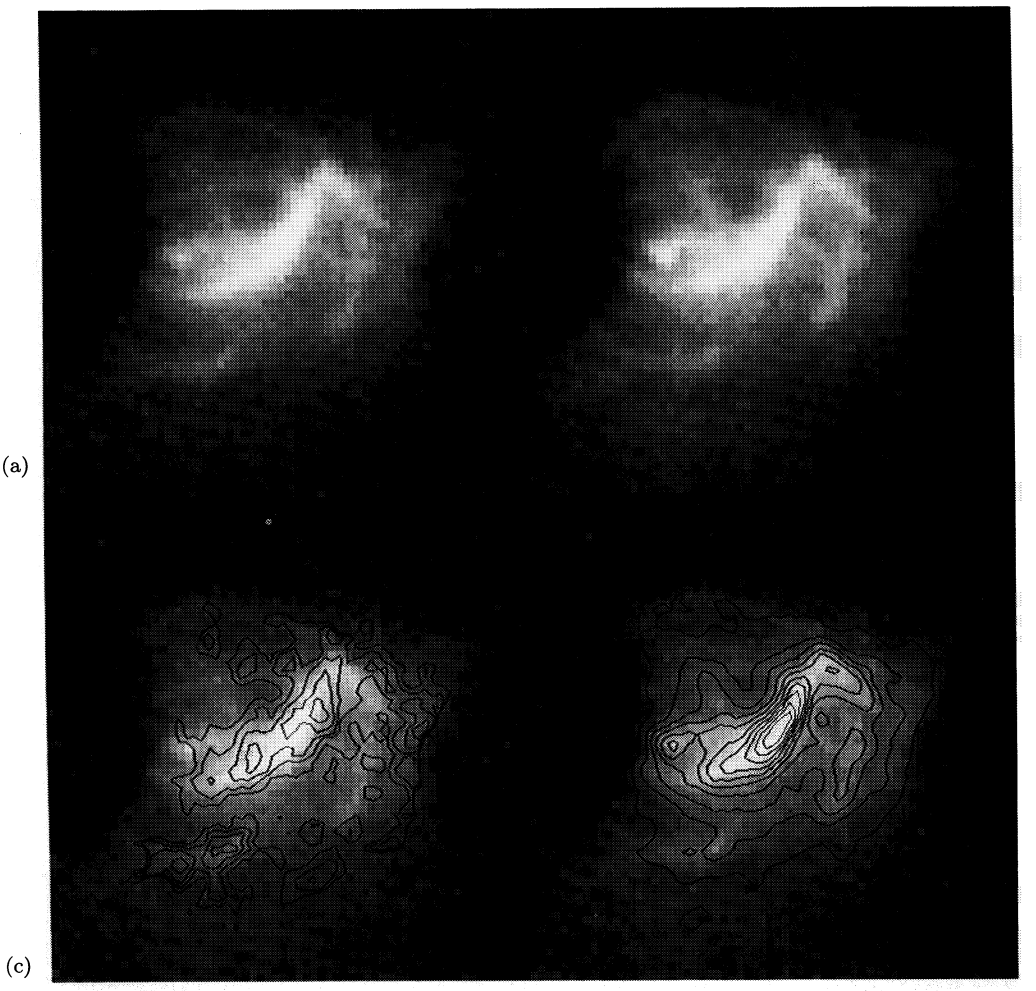

Fig. 4. Distribution of the temperature and emission measure overlaid on the X-ray image. (a) Be filter image (top left), (b) Al filter image (top right), (c) Temperature contour map (bottom left) overlaid on the X-ray image with the contour levels of 5.1, 5.3, 5.5, 5.7, 5.9 $\times 10^6$ K from the outside. (d) Emission measure (bottom right); the contour levels are 5 to 50 every 5 steps $\times 10^{27}$ cm^{-5} from the outside.

throughout the active region and that the temperature of the plasma may extend to 5–6 $\times$ 10^6 K, irrespective of the degree of brightness.

The SXT images show similar morphological features to the coronal green line (Fe XIV 5303 Å) images taken with the coronagraph at the Norikura Solar Observatory of NAOJ at the site of active regions. We have compared the temperature and emission measure derived from SXT images with AlMgMn/Al0.1 with those from a 5303 Å image for another active region, NOAA 6925, on 1991 November 16, and found a temperature of $T_{\rm SXT} = 2.3 \times 10^6$ K and emission measure of $EM_{\rm SXT} = 1.5 \times 10^{28}$ cm^{-5}, $T_{5303} = 2 \times 10^6$ K, and $EM_{5303} = 2 \times 10^{28}$ cm^{-5}. This indicates that the AlMgMn/Al0.1 pair can be used for temperature analyses of the normal component of active regions. Since there were no data taken with thick filters on that day, we cannot directly compare the emission measures around 2×10^6 K with that of 5×10^6 K.

The SXT temperatures from AlMgMn/Al0.1 derived above are lower than those of NOAA 6919. However, we cannot say that there is no high-temperature plasma in the region, since there is the case in which NOAA 6921 had a hot component of $T_{\rm Be/Al12} = 4.9 \times 10^6$ K, even though the normal component was lower, as $T_{\rm AlMgMn/Al0.1} = 2.4 \times 10^6$ K. The emission measure of the normal component is about 4-times larger than that of the hot component. This tendency seems to exist in most active regions, and is similar to the results of the Skylab observations with spectrometers (Pye et al. 1978; Levine and Pye 1980). Since if we define the value of Z as

$$Z \equiv \sqrt{\frac{EM_{\rm N}}{EM_{\rm H}}} \cdot \frac{T_{\rm N}}{T_{\rm H}} \simeq \frac{(nT)_{\rm N}}{(nT)_{\rm H}}, \quad (7)$$

where suffix N denotes the normal component around 2–3 $\times$ 10^6 K derived from the ratio of AlMgMn/Al0.1 and H denotes the hot component from Be/Al12, several cases of Z are Z(NOAA 6919 region A) = 0.80, Z(NOAA 6919 region B) = 0.84, and Z(NOAA 6921) = 0.91, the tendency may indicate a pressure-balance situation. This means that the energy content of the hot component may be energetically equivalent compared with the normal component.

The authors would like to thank Prof. Y. Ogawara, the Institute of Space and Astronautical Science, Profs. T. Hirayama and T. Kosugi, Drs. T. Watanabe and K. Ichimoto, National Astronomical Observatory of Japan, Dr. H. Hudson, University of Hawaii, for their suggestions during the course of the analysis.

References

Gerassimenko, M., and Nolte, J. T. 1978, *Solar Phys.*, **60**, 299.

Hara, H. 1992, Master thesis, Department of Astronomy, The University of Tokyo.

Levine, R. H., and Pye, J. P. 1980, *Solar Phys.*, **66**, 39.

Mewe, R., Gronenschild, E. H. B. M., and van den Oord, G. H. J. 1985, *Astron. Astrophys. Suppl.*, **62**, 197.

Mewe, R., Lemen, J. R., and van den Oord, G. H. J. 1986, *Astron. Astrophys. Suppl.*, **65**, 511.

Pye, J. P., Evans, K. D., Hutcheon, R. J., Gerassimenko, M., Davis, J. M., Krieger, A. S., and Vesecky, J. F. 1978, *Astron. Astrophys.*, **65**, 123.

Raymond, J. C., and Doyle, J. G. 1981, *Astrophys. J.*, **247**, 686.

Thomas, R. J., Starr, R., and Crannell, C. J. 1985, *Solar Phys.*, **95**, 323.

Tsuneta, S., Acton, L., Bruner, M., Lemen, J., Brown, W., Caravalho, R., Catura, R., Freeland, S., Jurcevich, B., Morrison, M., Ogawara, Y., Hirayama, T., and Owens, J. 1991, *Solar Phys.*, **136**, 37.

Vaiana, G. S., Krieger, A. S., and Timothy, A. F. 1973, *Solar Phys.*, **32**, 81.